

The RHIC optically-pumped polarized H⁺ ion source

A. Zelenski, S. Kokhanovski, A. Kponou, J. Ritter, V. Zubets

*Presented at PSTP2007: The International Workshop on Polarized Ion Sources,
Targets, and Polarimetry*

Brookhaven National Laboratory, Upton, NY
September 10-14, 2007

March 2008

Collider-Accelerator Department

Brookhaven National Laboratory

P.O. Box 5000

Upton, NY 11973-5000

www.bnl.gov

Notice: This manuscript has been authored by employees of Brookhaven Science Associates, LLC under Contract No. DE-AC02-98CH10886 with the U.S. Department of Energy. The publisher by accepting the manuscript for publication acknowledges that the United States Government retains a non-exclusive, paid-up, irrevocable, world-wide license to publish or reproduce the published form of this manuscript, or allow others to do so, for United States Government purposes.

This preprint is intended for publication in a journal or proceedings. Since changes may be made before publication, it may not be cited or reproduced without the author's permission.

DISCLAIMER

This report was prepared as an account of work sponsored by an agency of the United States Government. Neither the United States Government nor any agency thereof, nor any of their employees, nor any of their contractors, subcontractors, or their employees, makes any warranty, express or implied, or assumes any legal liability or responsibility for the accuracy, completeness, or any third party's use or the results of such use of any information, apparatus, product, or process disclosed, or represents that its use would not infringe privately owned rights. Reference herein to any specific commercial product, process, or service by trade name, trademark, manufacturer, or otherwise, does not necessarily constitute or imply its endorsement, recommendation, or favoring by the United States Government or any agency thereof or its contractors or subcontractors. The views and opinions of authors expressed herein do not necessarily state or reflect those of the United States Government or any agency thereof.

The RHIC Optically-Pumped Polarized H⁻ Ion Source.

A.Zelenski, S. Kokhanovski, A. Kponou, J. Ritter, V. Zubets

Brookhaven National Laboratory, Upton, NY, 11967

Abstract. The depolarization factors in the multi-step spin-transfer polarization technique and basic limitations on maximum polarization in the OPPIS (Optically-Pumped Polarized H⁻ Ion Source) are discussed. Detailed studies of polarization losses in the RHIC OPPIS and the source parameters optimization resulted in the OPPIS polarization increase to 86-90%. This contributed to increasing polarization in the AGS and RHIC to 65 ~ 70%.

Keywords: Polarized Ion Sources

PACS: 29.25.Lg

INTRODUCTION

Studies of polarized proton collisions in RHIC at energies of $\sqrt{s} = 200-500$ GeV provide unique opportunity for the proton spin structure studies and fundamental tests of QCD [1, 2]. RHIC is the first collider where the "Siberian snake" technique was very successfully implemented to avoid the resonance depolarization during beam acceleration in AGS and RHIC [3]. A luminosity of a $1.6 \cdot 10^{32} \text{ cm}^{-2} \text{ sec}^{-1}$ for polarized proton collisions in RHIC will be produced by colliding 120 bunches in each ring at $2 \cdot 10^{11}$ protons/bunch intensity. For the first time the intensity of the polarized beams produced in an optically pumped polarized H⁻ ion source was sufficient to charge RHIC to the maximum intensity limited by the beam-beam interaction.

The RHIC OPPIS produces routinely 0.5-1.0 mA (maximum 1.6 mA) current in 400 μs pulse duration. The polarized H⁻ ion beam (of 35 keV beam energy out of the source) is accelerated to 200 MeV in a linear accelerator for strip-injection to Booster. The 400 μs H⁻ ion pulse is captured in a single Booster bunch which contains about $4 \cdot 10^{11}$ polarized protons. Single bunch is accelerated in the Booster to 2.5 GeV energy and then transferred to the AGS, where it is accelerated to 24.3 GeV for injection to RHIC. The OPPIS initial longitudinal polarization is converted to the transverse direction while the beam passes two bending magnets. The second 47.4 deg. bending magnet switches injection between polarized and unpolarized (of about 100 mA intensity) H⁻ ion beam.

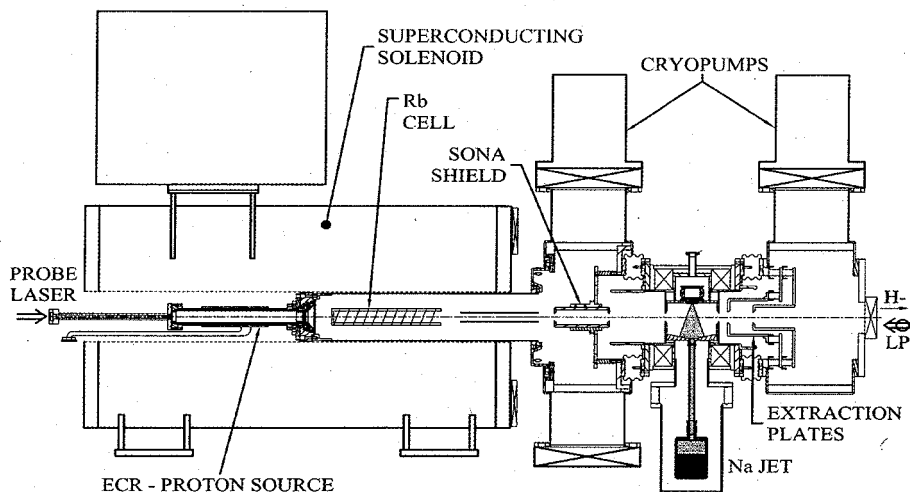


FIGURE 1. General layout of the RHIC OPPIS.

The magnet is pulsed and either beam can be accelerated pulse-to-pulse in the same RFQ. A pulsed focusing solenoid in front of the RFQ is tuned for the optimal (for either beam) transmission. It rotates the polarization direction for about 360 degrees, but still keeps it in the transverse plane, and a final polarization alignment to the vertical direction can be adjusted by a spin-rotator solenoid in the 750 keV beam transport line before injection to the linac [2]. The AGS cycle for polarized beam operation is 3 seconds. The OPPIS operates at 1 Hz repetition rate and additional source pulses are directed to a 200 MeV p-Carbon polarimeter by a pulsed bending magnet in the high-energy beam transport line (for continuous polarization monitoring). The spin-rotator tuning is done using vertical polarimeter arms.

In the OPPIS an ECR-type source produces a primary proton beam of 2.8 - 3.0 keV energy, which is converted to electron-spin polarized H atoms by electron pick-up in an optically pumped Rb vapor cell. Electrostatic deflection plates downstream of the polarized alkali remove any residual H^+ or other charged species. The electron-polarized H beam then passes through a magnetic field reversal region, where the polarization is transferred to the nucleus, via hyperfine interaction (Sona-transition). The polarized H atoms are then negatively ionized in a Na-jet vapor cell to form nuclear polarized H-ions (see Fig. 1). Alternatively, the H atoms can be ionized in a He gaseous cell to form polarized protons. This source is capable of producing in excess of 1.6 mA polarized H^- ion current in dc operation [1].

The OPPIS technique is a multi-step polarization-transfer process. At each step there is some loss of polarization, which can be expressed as follows:

$$P = P_{RB} \cdot S \cdot B_{H2} \cdot E_{LS} \cdot E_{SONA} \cdot E_{ION} \cdot M \cdot X,$$

where P_{RB} is an average Rb vapor polarization, S - represents the degree of matching between the Rb polarization profile and the spatial proton beam profile, B_{H2} is a factor accounting for proton neutralization on residual hydrogen from the ECR source,

P_{Rb} – Rb vapor polarization	0.99 - 0.99
S – spatial polarization distribution	0.98 - 0.98
B_{H2} – neutralization in residual gas	0.95 - 0.97
E_{LS} – spin-orbital interaction	0.98 - 0.98
E_{Sona} – Sona-transition efficiency	0.97 - 0.99
E_{ion} – losses in ionizer	0.95 - 0.98
M – molecular ions	0.98 - 1.00
X – unknown factors	1.00 - 1.00
Total	0.85 - 0.90

Table I. Polarization losses estimations.

E_{LS} accounts for spin-orbital depolarization of hydrogen atoms (produced in excited states), **E_{Sona}** is the efficiency of the Sona transition, **E_{ion}** is a polarization loss in the ionization process, **M** - accounts for polarization dilution by molecular H_2^+ ions produced in the ECR source, and **X** - represents other factors (for example polarization loss between source and 200 MeV polarimeter).

The detailed studies and optimization of each of these factors resulted in 86% polarization in Run 2006 and further increase to 88~90% in Run 2007 (see Table I). The polarization loss factors were discussed in earlier papers /2, 3/. Here we report the reduction of losses in the **B_{H2}**, **E_{Sona}** and **E_{ion}** factors.

B_{H2} -Proton neutralization in the residual hydrogen gas from the ECR source. The neutralization of the primary proton beam from the ECR source, in residual hydrogen gas upstream of and inside the Rb cell, produces unpolarized hydrogen atoms, which dilute polarization. The factor **B_{H2}** can be calculated from polarization and current measurements at low Rb vapor thickness, where the dilution factor is enhanced. It depends on the extraction grid and Rb cell geometry vacuum chamber conductance and pumping speed. A typical hydrogen flow in ECR source is about 0.1scc/s. With pumping speed of about 4000 l/s (produced by two cryogenic vacuum pumps) an operational vacuum in the Rb cell is about $2 \cdot 10^{-6}$ torr, which corresponds to hydrogen gas density of about $7 \cdot 10^{10}$ H_2/cm^3 (this density is higher inside the cell). The operational Rb vapor density is $2 \cdot 10^{12}$ atoms/s. The neutralization cross-section in Rb vapor (of a 10^{-14} cm^2) is about 10 times larger than neutralization cross-section in collisions with hydrogen molecules. This helps to suppress the dilution factor. Some neutralization occurs on the atomic and molecular hydrogen gas flowing along the Rb cell axis and can be reduced only by increasing the proton/neutral fraction ratio out of the ECR source. The recent optimization of the Rb cell and vacuum chamber geometry (the cell length was reduced from 30 cm to 20 cm and moved further downstream from the ECR source, and the cell support and cooling screen were redesigned to improve vacuum conductance) significantly reduced hydrogen gas density inside the Rb cell. This resulted in significant polarization gain at low Rb thicknesses (see Fig. 2).

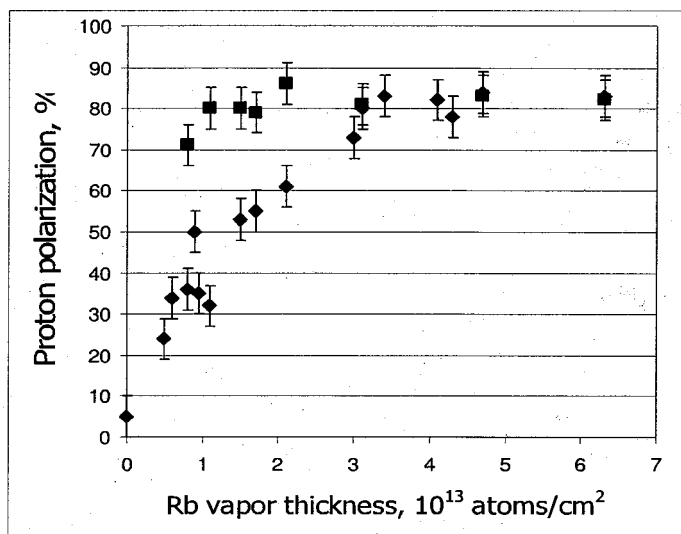


FIGURE 2. Proton polarization at 200 MeV vs. Rb vapor thickness: before (◆) and after (■) the Rb cell upgrade.

M-Polarization dilution by H_2^+ molecular ions. There exists a molecular H_2^+ ion component in the ECR ion source. In the OPPIS, molecular ions after dissociation will appear as H ions with the half of the primary beam energy. The polarization of this beam might be different from the main beam (measurement in Lamb-shift polarimeter gives about half the polarization for this molecular component). This component was observed at the TRIUMF OPPIS, but it was efficiently suppressed by electrostatic lenses in the 3 keV LEPT. In the RHIC OPPIS the H beam is accelerated for 32 keV immediately after ionization, producing 35 keV main beam and 33.5 keV beam from molecular ion admixture. These beams are not well separated in the LEPT, and the molecular component is responsible for polarization dilution. At lower acceleration energy these beams are separated, and the half energy component was directly observed (see Fig.3).

A value of molecular component of about 10-40 % was measured under different ECR conditions. Since every H_2^+ ion is dissociated to two half energy atoms, it means 5-20% molecular component out of the ECR-source. The molecular component increases at higher ECR extraction voltage. The H⁺ yield drops at atomic beam energy above 3.0 keV, but for half energy beam of a 1.5 – 2.0 keV the yield is at maximum value. It explains an increase of molecular component up to 40% at 4.0 keV ECR extraction energy, and correspondent polarization decrease, which was also observed in polarization measurements.

The increase of the ECR current was obtained earlier with an admixture of a few percent of gaseous oxygen to the hydrogen in the source [2]. The oxygen admixture also reduces the molecular H_2^+ ion production i.e. improves the dissociation ratio in the source. The magnetic field shape in the ECR region also affects the dissociation ratio. The optimization of the ECR source parameters gave rise to an increase of the main beam intensity and reduction of the half energy, lower polarization component to

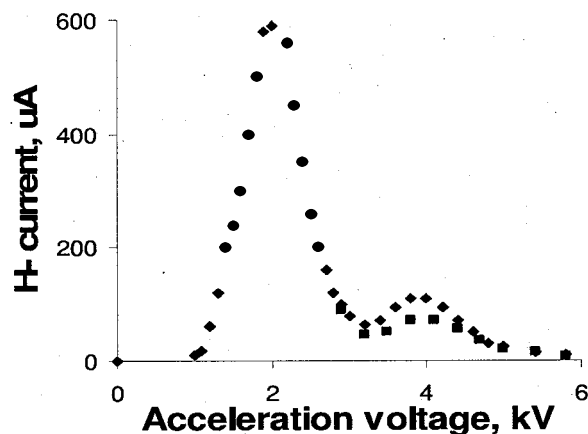


FIGURE 3. Molecular H_2^+ beam component is appeared as a second bump shifted to about a half primary ECR proton energy at a fixed bending magnet setting. Diamonds-dc operation; squares-pulsed operation.

below 10%. The ECR operation in a pulsed mode was also studied. Significant molecular component suppression was also observed in a pulsed operation, due to a difference in the rise time for main and half energy beam components. In a pulsed operation the molecular component is about 5%. The next step was a suppression of the lower energy component during acceleration to 35 keV after the ionizer and in the LEBT. The two-gap acceleration system was upgraded to three-gaps and the voltage in the first gap was tuned to suppress the half energy component. The voltages at the second and third gaps were adjusted to minimize the main component losses. The use of a single deceleration Einzel lens in LEBT also suppresses the lower energy component. The combined effect of these modifications is a significant (almost ten times) suppression of the beam transmission in LEBT for the lower energy molecular origin beam. As a result of these upgrades the estimated M factor was reduced to 0.98.

E_{Sona} -Sona-transition efficiency. The electron polarization is transferred to protons by the Sona-transition technique as the electron-spin polarized atomic H beam passes through a magnetic field reversal region in between high field “polarizer” solenoid and ionizer solenoid. Very strict restrictions are applied to the transverse magnetic field in the zero-crossing region (where the longitudinal field reverses direction) to avoid spin-flip [4]. The longitudinal field gradient generates a transverse field B_r : $B_r = r/2(dB/dz)$, and to fulfill Sona-transition conditions (for a \varnothing 2 cm atomic hydrogen beam) the $dB/dz \ll 0.2$ G/cm is required at the $B_z=0$ crossing point. A “soft” steel cylindrical Sona-shield and Correction Coil (CC) were designed and built to reduce the field gradient to less than 0.2 G/cm in the limited space between superconducting solenoid 25 kG field and ionizer solenoid 1.5 kG field. As a result of Sona-shield and correction coil optimization, the gradient was reduced to less than 0.09 G/cm (see Fig. 3, magnetic field calculations, which were confirmed by field measurements).

For the Sona-transition, efficiency studies and optimization the polarization dependence vs. correction coil current was measured in a wide range of CC field.

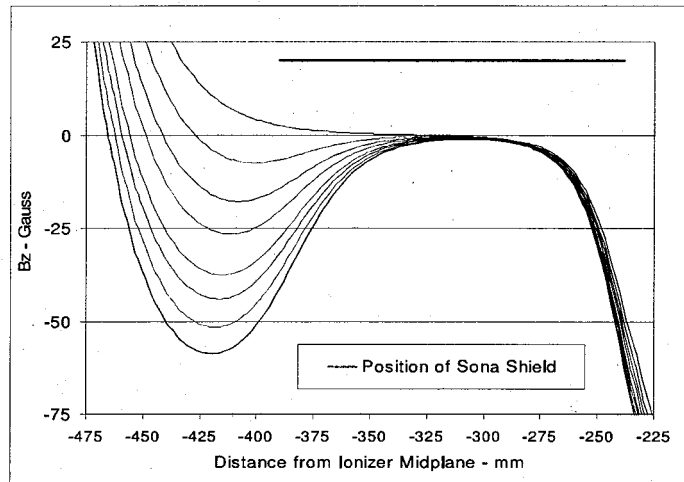


FIGURE 4. Calculated magnetic field profiles in the Sona transition region for several correction coil currents corresponding to polarization oscillation peaks.

Polarization was measured in the Lamb-shift polarimeter at 35 keV beam energy and at 200 MeV in the p-Carbon polarimeter. Typical results are presented in Fig. 4. Since the CC field direction is opposite to superconducting solenoid field, the zero-crossing point is moving inside the Sona-shield upstream, when CC current is increased. This reduces the gradient and slightly increases polarization. At some current value the zero-crossing point is pushed out of the shield and the gradient is greatly increased (see Fig.4), which causes a steep polarization drop.

This is an expected result and it was observed in previous experiments at the TRIUMF OPPIS /2/ and initial tests at the RHIC OPPIS. A new, stronger, correction coil (and additional magnetic shield at the superconducting solenoid flange) allowed significant expansion of the field variation range, which revealed unexpected periodic polarization quantum oscillations. The polarization almost completely recovered at higher CC field, and the oscillations have a period of about 5 A correction coil current increment. The amplitude of the oscillations is slowly decreased with higher CC field. To further explore this effect, the CC field was reversed. This pushed the zero-crossing upstream outside of the shield, and the polarization oscillations were also observed. The field gradients at zero-crossing region were calculated. The resonance-like polarization oscillations are going through maximum with an increment of about 5 G/cm. An atom passing the field reversal region at 1 cm off axis will “see” about 2.5 G transverse magnetic field. The Larmor electron spin precession in this field will be: $\omega \cdot B \cdot t = 2\pi \cdot 28 \cdot 10^9 \text{ B} \cdot t$. The precession time t is the atom travel time through zero-crossing region of about 5 cm long, which for 3.0 keV atoms (at speed $7 \cdot 10^7 \text{ cm/s}$) is equal to: $t \sim 1.4 \cdot 10^{-7} \text{ s}$. This gives: $\omega \cdot B \cdot t \approx 2\pi$, which give rise to the double spin flip in between polarization maximums and single spin flip when polarization drops to minimum. This transverse field induces the spin-flip for only one of two electron spin polarized atomic hydrogen state: $\langle 1 \rangle = (m_j=1/2, m_l=1/2)$.

The other “mixed” state: $\langle 2 \rangle = [(m_j=1/2, m_l=-1/2) + (m_j=1/2, m_l=+1/2)]$ - adiabatically follows the reversing field direction. Also there is the radial field distribution and spin flip conditions are different for atoms at different radii. This affects the amplitude of polarization oscillations, which can vary between 15-50 % for

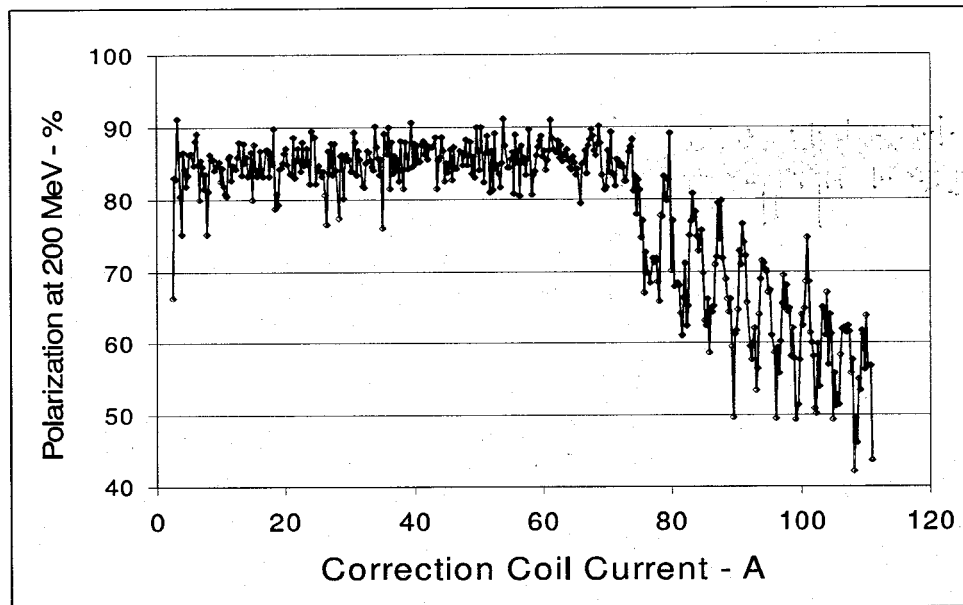


FIGURE 5. H Polarization measured in the 200 MeV polarimeter. Sona-shield collimator diameter – 2.0 cm, ionizer solenoid field 1.9 kG.

different Sona transition configurations. The stronger radial dependence at higher field gradients reduces the coherency of spin flip, which decreases both the polarization and the oscillation amplitude (see Fig. 5).

The minimal field gradient and maximum polarization is obtained just before the field dip, providing that all the other transverse field sources are eliminated by the Sona shield (an additional μ -metal shield layer was inserted inside the “soft” steel cylinder to suppress the small residual field of the steel itself). The polarizations for different beam diameters – 1.2 cm, 1.6 cm and 2.0 cm (beam diameter is defined by the collimator at the entrance of Sona-shield) were measured after this optimization and within the errors the maximum polarization values are the same. This means that Sona-transition efficiency is close to 100% (the best value for further estimations is: $E_{\text{Sona}} = 0.99 \pm 0.01$).

E_{ion} -Polarization losses in Na-jet ionizer cell. A magnetic field of about 1.5 kG is required in the sodium-jet ionizer cell to break the electron-proton hyperfine interaction. Since the critical field for hydrogen atoms is 507.6 G, the theoretical polarization loss at this field is about 3%. The ionizer field increase over 1.5 kG is not very effective for polarization increase (the theoretical polarization gain between 1.5 kG and 2.0 kG is only ~1%) but it will cause beam emittance growth beyond the RFQ acceptance and result in beam intensity losses.

Significantly larger polarization increase at higher ionizer fields was observed in experiments (see Fig.5). Similar results were also observed in earlier measurements at the TRIUMF OPPIS [2], but it was explained by sodium vapor penetration in the low field region (in the oven-type sodium cell) and possible ionizer field influence on the Sona-transition region. In the present experiments, the sodium vapor is very well confined in the jet-cell within the center flattop field region. For every ionizer field

strength value the correction coil scan was done to optimize the Sona-transition. The measurements were repeated with a smaller 1.2 cm diameter beam, which would reduce the possible additional contribution of the spatial polarization distribution (since the central fraction of the beam is better transported and accelerated in the linac to the 200 MeV polarimeter). Still, the polarization increase at higher field is not accounted by hyperfine interaction breaking alone (see Fig.6). This means that there is another effect, which also depends on the ionizer field strength. One possible explanation might be an observed effect of polarization dependence on the Na-jet vapor thickness.

Usually the jet cell is operated at sodium reservoir temperature of $\sim 500^\circ\text{C}$, which is required for the H^- ion yield saturation (the estimated total jet thickness is $\sim 2 \cdot 10^{15}$ atoms/cm 2). At 470°C temperature, where the H^- current drops to about 80% of maximum and thickness is reduced to $\sim 1.0 \cdot 10^{15}$ atoms/cm 2 the polarization is increased for $\sim 2\text{-}3\%$. Multiple charge-exchange processes are more likely at high sodium vapor thickness, which might cause some depolarization at each collision. The stronger ionizer field would suppress this depolarization process and reduce polarization losses. The factor E_{ion} is presently estimated at: $E_{\text{ion}} \sim 0.97\text{-}0.98$ (for ionizer field of 1.5-2.0 kG). The benefit of the higher ionizer field for increasing polarization is partially offset by beam intensity reduction due to emittance growth, which is proportional $\sim BR^2$. For the typical RFQ acceptance of about 2.0π mm-mrad this limits the beam radii to less than ~ 0.8 cm, and ionizer magnetic field to less than 2.0 kG. A higher brightness polarized atomic H beam is required to keep beam emittance in the RFQ acceptance range at high field by using smaller diameter collimated beam.

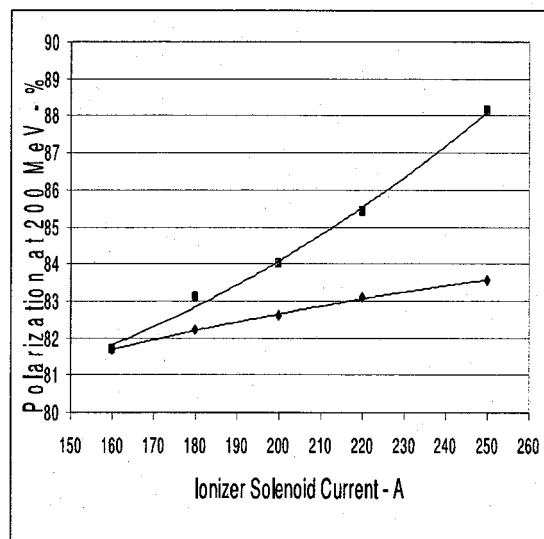


FIGURE 6. Measured (■) and calculated (◆) polarization vs. ionizer solenoid field strength. Ionizer field at 250 A current is equal to 1.98 kG.

OPPIS with the "Fast Atomic Hydrogen Beam Source".

The ECR proton source is operated in high magnetic field. It has low hydrogen gas consumption, which makes possible a dc OPPIS operation with intensity in excess of 1.0 mA. This intensity is two orders of magnitude higher than dc atomic beam sources /1/. However, the ECR source has a comparatively low emission current density and high beam divergence. This limits further current increase and gives rise to inefficient use of the available laser power for optical pumping. In fact only about 15% of the electron-spin polarized hydrogen atoms produced in Rb cell is within the ionizer cell acceptance.

In pulsed operation, suitable for application at high-energy accelerators and colliders, the ECR source limitations can be overcome by using instead a high brightness proton source outside the magnetic field /6/. Following neutralization in hydrogen, the high brightness 3.0- 4.0 keV atomic H beam is injected into a superconducting solenoid, where both a He ionizer cell and an optically-pumped Rb cell are situated in the same 25-30 kG solenoid field, which is required to preserve the electron-spin polarization. The injected H atoms are ionized in the He cell with 80% efficiency to form a low emittance intense proton beam, which enters the polarized Rb vapor cell (see Fig. 7).

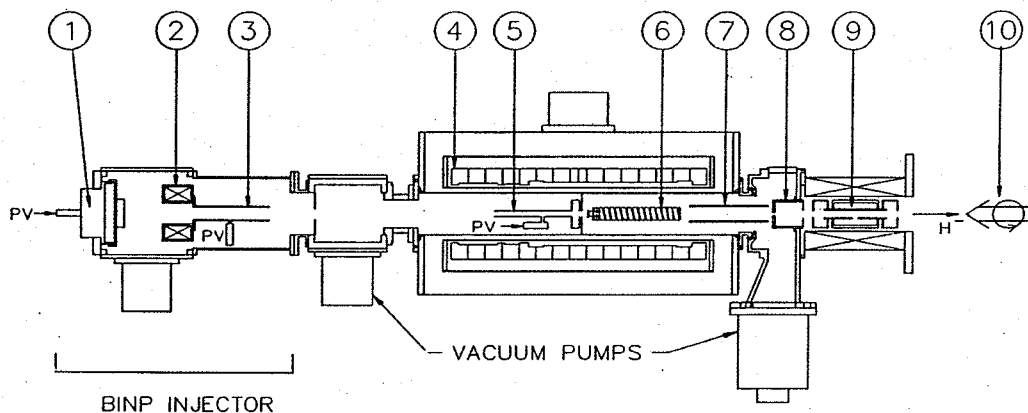


FIGURE 7. Layout of the OPPIS with atomic hydrogen injector: 1-high-brightness proton source; 2-focussing solenoid; 3-pulsed hydrogen neutralization cell; 4-super conducting solenoid 30 kG; 5-Pulsed He ionizer cell; 6-optically-pumped Rb cell; 7-deflecting plates; 8-Sona shield; 9-sodium ionizer cell; 10-pulsed laser. beam.

The protons pick up polarized electrons from the Rb atoms to become a beam of electron-spin polarized H atoms. A negative bias of about 1.0 kV applied to the He cell decelerates the proton beam produced in the cell. This allows energy separation of the polarized hydrogen atoms produced after lower energy proton neutralization in Rb vapor and residual hydrogen atoms of the primary beam. Atomic hydrogen beam current densities greater than 100 mA/cm² can be obtained at the Na jet ionizer location (about 180 cm from the source) by using a very high brightness fast atomic beam source developed at BINP, Novosibirsk /7/, and tested in experiments at TRIUMF, where more than 10 mA polarized H⁺ and 50 mA proton beam intensity was demonstrated /1/.

Higher polarization is also expected with the fast atomic beam source due to: a) elimination of neutralization in residual hydrogen - $B_{H2} \sim 1$; b) better Sona-transition transition efficiency for the smaller ~ 1.5 cm diameter beam; c) use of higher ionizer field (up to 3.0 kG), while still keeping the beam emittance below 2.0π mm·mrad, because of the smaller beam – 1.5 cm diameter. All these factors combined will further increase polarization in the pulsed OPPIS to over 90% and the source intensity to over 10 mA.

The ECR-source replacement with an atomic hydrogen injector will provide the high intensity beam for polarized RHIC luminosity upgrade and for future eRHIC facilities.

The authors are thankful to Prof. T. Clegg, UNC and TUNL, for very helpful discussions of Sona transition features and the observed polarization oscillations.

REFERENCES

1. A. Zelenski, Proc.SPIN2000, **AIP 570**, p.179, (2000).
2. A. Zelenski et al., **NIM A334**, p.285, (1993).
3. A. Zelenski et al., SPIN2002, **AIP 675**, p.881, (2003).
5. P. G. Sona, *Energia Nucl.*, **14**, p.295, (1967).
6. A. Zelenski et al., **NIM A245**, p.223, (1986).
7. V. Davydenko, **NIM A427**, p.230, (1999).